Synthesis and Characterization of One-Dimensional Polymeric Chlorocadmate(II) Systems

A. Bonamartini Corradi,* S. Bruckner, M. R. Cramarossa, T. Manfredini, L. Menabue, and M. Saladini

Dipartimento di Chimica, Facoltà di Ingegneria, University of Modena, 41100 Modena, Italy

A. Saccani and F. Sandrolini

Dipartimento di Chimica Applicata e Scienza dei Materiali, Facoltà di Ingegneria, University of Bologna, 40136 Bologna, Italy

J. Giusti

Dipartimento di Chimica, University of Florence, 50100 Florence, Italy

Received July 28, 1992. Revised Manuscript Received October 23, 1992

In this paper we report the synthesis and the structural, thermal, electrical properties of 1-D polymeric chlorocadmates(II), having *N*-methylpropane-1,3-diammonium ($mepnH_2$) and *N,N*-diethylpropane-1,3-diammonium (et_2pnH_2) as countercations. The $(mepnH_2)_2[Cd_3Cl_{10}]$ crystallizes in space group $P2_1/c$. The unit cell dimensions are a = 10.164 (3) Å, b = 13.434 (10) Å, c = 10.099 (3) Å, β = 112.04 (3)°, V = 1278 (1) Å^3, Z = 2. The final R value for 2124 reflections ($I > 2\sigma(I)$) is 0.0445 (R_w = 0.0384). Its structure consists of *N*-methylpropane-1,3-diamine dications and infinite chains of $[(Cd_3Cl_{10})_n^{4n-}]_n$ moieties forming 1-D polymer running along the x axis. The $(et_2pnH_2)_2[Cd_5Cl_{14}]\cdot 2H_2O$ crystallizes in space group $P\bar{1}$. The unit cell dimensions are a = 6.874 (1) Å, b = 10.381 (1) Å, c = 14.572 (1) Å, α = 100.14 (1)°, β = 99.31 (1)°, γ = 97.46 (1)°, V = 996.7 (2) Å^3, Z = 1. The final R value for 3405 reflections ($I > 2\sigma(I)$) is 0.0452 (R_w = 0.0393). Its structure consists of *N,N*-diethylpropane-1,3-diamine dications, infinite alternate stacked pseudoplanar trinuclear $[Cd_3Cl_8]^{2-}$ and dinuclear $[Cd_2Cl_6]^{2-}$ dianions and uncoordinated water molecules. Both the packings are strengthened by N-H···Cl hydrogen bonds between anions and cations. A first-order phase transition of $(mepnH_2)_2[Cd_3Cl_{10}]$ has been identified by DSC measurements and X-ray powder diffraction, related to the disordering of the hydrocarbon chains at high temperature. This increases the cell volume. The electrical conductivity of the compounds can be envisaged as protonic, and the whole electrical behavior can be correlated to their structures and phase transition.

Introduction

Halocadmates(II) are particularly suitable systems for designing the construction of unusual structural archetypes, from which peculiar thermal, catalytic, electrical, and polymorphic properties can arise. This is due to the fact that the Cd^{2+} ion, being a d^{10}, exhibits a great variety of coordination numbers and geometries, depending on crystal packing and hydrogen bonding, as well as halide dimensions.[1,2] In particular, two-dimensional polymeric chlorocadmates(II) have received a great deal of attention from both the theoretical and experimental points of view, representing appropriate model systems for the prediction of impurity electronic configurations and their lattice locations, which is a key problem in semiconductor physics.[3-5]

In spite of the widely studied two-dimensional polymeric chlorocadmates(II), much less is known about one-dimensional linear chain compounds, since this type of structure seems to be rather unusual for a Cd(II) ion.[2,6] To fill this gap, we previously synthesized and investigated the properties of some polymeric 1-D linear chain chlorocadmates(II) having cyclic saturated mono-, di-, or triammonium cations, as countercations.[7-9]

In the present paper we report on the synthesis and the structural, thermal, spectroscopic, and electrical characterizations of two other polymeric one-dimensional chlorocadmate(II) systems of substituted diprotonated propane-1,3-amines, namely, *N*-methyl and *N,N*-diethyl derivatives, [(hereafter abbreviated as $mepnH_2$ and et_2pnH_2, respectively)] of formula $(mepnH_2)_2[Cd_3Cl_{10}]$ and $(et_2pnH_2)_2[Cd_5Cl_{14}]\cdot 2H_2O$.

The present results, compared with those previously obtained for one-dimensional linear chain chloro-

(1) Dean, P. A. W. *Prog. Inorg. Chem.* **1978**, *24*, 109 and references therein.
(2) Tuck, D. G. *Rev. Inorg. Chem.* **1979**, *1*, 209 and references therein.
(3) Mokhlisse, R.; Couzi, M.; Chanh, N. B.; Haget, Y.; Hauw, C.; Meresse, A. *J. Phys. Chem. Solids* **1985**, *46*, 187.
(4) Chanh, N. B.; Hauw, C.; Meresse, A.; Rey-Lafon, M.; Ricard, L. *J. Phys. Chem. Solids* **1985**, *46*, 1413 and references therein.
(5) Bensekrane, M.; Goltzene, A.; Meyer, B.; Schwab, C.; Elwell, D.; Feigelson, R. S. *J. Phys. Chem. Solids* **1985**, *46*, 481 and references therein.
(6) Bart, J. C. J.; Bassi, I. W.; Calcaterra, M. *Acta Crystallogr.* **1980**, *B36*, 2616 and references therein.
(7) Manfredini, T.; Pellacani, G. C.; Battaglia, L. P.; Bonamartini Corradi, A.; Motori, A.; Saccani, A.; Sandrolini, F. *Mater. Chem. Phys.* **1988**, *20*, 215.
(8) Manfredini, T.; Pellacani, G. C.; Battaglia, L. P.; Bonamartini Corradi, A.; Giusti, J.; Motori, A.; Saccani, A.; Sandrolini, F. *Mater. Chem. Phys.* **1989**, *24*, 25.
(9) Battaglia, L. P.; Bonamartini Corradi, A.; Pelosi, G.; Cramarossa, M. R.; Manfredini, T.; Pellacani, G. C.; Motori, A.; Saccani, A.; Sandrolini, F.; Giusti, J. *Mater. Eng.* **1990**, *1*, 537.

0897-4756/93/2805-0090$04.00/0

Table I. Experimental Data for the Crystallographic Analysis of the Compounds

	$(mepnH_2)_2[Cd_3Cl_{10}]$	$(et_2pnH_2)_2[Cd_5Cl_{14}]\cdot 2H_2O$
mol formula	$C_8H_{28}Cd_3Cl_{10}N_4$	$C_{14}H_{44}Cd_5Cl_{14}N_4O_2$
mol wt	872.06	1358.68
space group	$P2_1/c$	$P\bar{1}$
a/Å	10.164 (3)	6.874 (1)
b/Å	13.434 (10)	10.381 (1)
c/Å	10.099 (3)	14.572 (1)
α/deg		100.14 (1)
β/deg	112.04 (3)	99.31 (1)
γ/deg		97.46 (1)
V/Å^3	1278 (1)	996.7 (2)
Z	2	1
d_{calcd}/g cm^{-3}	2.27	2.26
d_{obs}/g cm^{-3}	2.24	2.25
cryst size/mm	0.30 × 0.35 × 0.32	0.35 × 0.20 × 0.25
radiation (λ, Å)	Mo Kα (λ = 0.710 69)	
θ limits/deg.	2.5–25	
temp/°C	25	
μ(Mo Kα)/cm^{-1}	35.3	35.9
F(000)	836	650
reflns collected	2496	3659
unique data used ($I > 2\sigma(I)$)	2124	3405
R	0.0445	0.0452
R_w	0.0384	0.0393

cadmates(II),[7-9] enable us to outline a consistent and reasonable picture of the factors controlling these types of stereochemistries and their polymeric nature. These results also allow us to correlate their symmetry, thermal, optical, and electrical behavior.

Further interest arises from the fact that these materials represent unusual solid inorganic/organic composites which, as they exhibit a wide variety of interesting properties, could be very useful for future application as engineering materials. This allows what has been called "crystal lattice engineering" to be practised on a specific class of compounds.

Experimental Section

Synthesis. Both the compounds were prepared by mixing the appropriate amines and $CdCl_2\cdot 2H_2O$ (molar ratios from 1:1 to 1:3) in concentrated hydrogen chloride solutions (37%). By slow evaporation of the solutions at room temperature over some days white crystals resulted suitable for X-ray single-crystal diffraction. All compounds are stable in air at room temperature. Elemental analyses: $(mepnH_2)_2[Cd_3Cl_{10}]$ found C = 11.05%; H = 3.26%; N = 6.39%; calcd for $C_8H_{28}N_4Cl_{10}Cd_3$ C = 11.01%; H = 3.24%; N = 6.42%. $(et_2pnH_2)_2[Cd_5Cl_{14}]\cdot 2H_2O$: found C = 12.40%; H = 3.25%; N = 4.12%; calcd for $C_{14}H_{44}N_4O_2Cl_{14}Cd_5$ C = 12.36%; H = 3.26%; N = 4.12%.

The $(et_2pnH_2)_2[Cd_5Cl_{14}]$ compound was obtained from the hydrated form by heating at 100 °C for 2 h. Elemental analyses: $(et_2pnH_2)_2[Cd_5Cl_{14}]$ found C = 12.68%; H = 3.06%; N = 14.22%; calcd for $C_{14}H_{40}N_4Cl_{14}Cd_5$ C = 12.70%; H = 3.05%; N = 4.23%.

Physical Measurements. Thermogravimetric and differential scanning calorimetric analyses were performed respectively with a Mettler thermobalance and a Perkin-Elmer DSC-7 calorimeter equipped with IBM PS 2/30 automatic data acquisition and processing software, employing sealed Al pans. Far-infrared spectra were recorded with an FT-IR Brucker spectrophotometer in polyethylene pellets in the 500–60-cm^{-1} spectral range. Carbon, hydrogen, and nitrogen were analyzed with a Carlo Erba MOD 1106 elemental analyzer.

X-ray Crystallographic Data. The structures were determined using an ENRAF-Nonius CAD4 single-crystal diffractometer. Lattice constants were determined by least-squares refinement of the angular setting of 25 reflections. Crystal data details are summarized in Table I. Intensity data were collected by using Mo Kα radiations with the ω-2θ scan technique in the 2.5–25° θ range with scan speed 1.1–8.2° min^{-1} for complex $(mepnH_2)_2[Cd_3Cl_{10}]$ and 1.3–8.2 for complex $(et_2pnH_2)_2[Cd_5Cl_{14}]\cdot 2H_2O$. All data were corrected for Lorentz and polarization effects. The structures were solved by conventional Patterson and Fourier technique and refined through full-matrix least-squares calculations. Anisotropic refinements were carried out for non-hydrogen atoms. Subsequent ΔF maps provided the position of nine hydrogen atoms for $(mepnH_2)_2[Cd_3Cl_{10}]$ and five for $(et_2pnH_2)_2[Cd_5Cl_{14}]\cdot 2H_2O$, which were treated as fixed contributors together with the remaining hydrogen atoms fixed at their calculated positions. Further refinement of this model gives R index of 0.0445 (R_w = 0.0384) using the weighting scheme $w = 169.30/(\sigma^2F_0 + 0.0005F_0^2)$ for complex $(mepnH_2)_2[Cd_3Cl_{10}]$ and R index of 0.0452 (R_w = 0.0393) using unit weight for complex $(et_2pnH_2)_2[Cd_5Cl_{14}]\cdot 2H_2O$. In the final refinement 15 reflections for $(mepnH_2)_2[Cd_3Cl_{10}]$ and 23 for $(et_2pnH_2)_2[Cd_5Cl_{14}]\cdot 2H_2O$ were excluded because affected by extinction or counting errors. Complex neutral scattering factors[10] were used throughout; all calculations were carried out on a VAX 6310 computer of the Centro Interdipartimentale di Calcolo Automatico ed Informatica Applicata (CICAIA) of the University of Modena by using SHELX76,[11] PARST,[12] and ORTEP[13] programs. Final fractional coordinates for non-hydrogen atoms are listed in Tables II and III for complexes $(mepnH_2)_2[Cd_3Cl_{10}]$ and $(et_2pnH_2)_2[Cd_5Cl_{14}]\cdot 2H_2O$, respectively.

X-ray powder diffraction analysis for the calculation of structural parameters of the high temperature $(mepnH_2)_2[Cd_3$-

Table II. Fractional Atomic Coordinates for Non-Hydrogen Atoms for $(mepnH_2)_2[Cd_3Cl_{10}]$

atom	x/a	y/b	z/c
Cd(1)	0.0	0.0	0.0
Cd(2)	0.29478 (3)	0.01094 (3)	−0.08668 (3)
Cl(1)	0.2625 (1)	−0.05849 (9)	0.1405 (1)
Cl(2)	0.1093 (1)	0.15250 (8)	−0.0683 (1)
Cl(3)	0.4846 (1)	−0.12503 (8)	−0.0730 (1)
Cl(4)	0.2978 (1)	0.09120 (9)	−0.3088 (1)
Cl(5)	0.0544 (1)	−0.09497 (9)	−0.2209 (1)
N(1)	0.5395 (4)	−0.1925 (3)	0.6470 (4)
N(2)	0.0220 (4)	−0.1751 (4)	0.4370 (5)
C(1)	0.6811 (5)	−0.1608 (4)	0.6477 (6)
C(2)	0.4180 (5)	−0.1368 (3)	0.5436 (5)
C(3)	0.2798 (5)	−0.1812 (4)	0.5432 (5)
C(4)	0.1539 (5)	−0.1257 (4)	0.4410 (5)

Table III. Fractional Atomic Coordinates for Non-Hydrogen Atoms for $(et_2pnH_2)_2[Cd_5Cl_{14}]\cdot 2H_2O$

atom	x/a	y/b	z/c
Cd(1)	0.0	0.0	0.0
Cd(2)	0.11912 (6)	0.14076 (4)	0.27612 (3)
Cd(3)	−0.43843 (5)	0.06477 (4)	0.13807 (3)
Cl(1)	−0.3590 (2)	−0.1322 (1)	0.01398 (9)
Cl(2)	−0.0894 (2)	0.1970 (1)	0.1160 (1)
Cl(3)	0.2000 (2)	−0.0676 (1)	0.14535 (9)
Cl(4)	−0.2300 (2)	−0.0105 (1)	0.27556 (9)
Cl(5)	0.4642 (2)	0.2521 (1)	0.2484 (1)
Cl(6)	0.2752 (2)	0.0342 (1)	0.4096 (1)
Cl(7)	0.0700 (2)	0.3529 (1)	0.3749 (1)
N(1)	0.2927 (7)	0.7779 (5)	0.5387 (3)
N(2)	0.6228 (7)	0.6467 (4)	0.2701 (3)
C(1)	0.3791 (9)	0.6697 (5)	0.4881 (4)
C(2)	0.4140 (8)	0.7006 (6)	0.3932 (4)
C(3)	0.5276 (9)	0.6001 (6)	0.3463 (4)
C(4)	0.4749 (9)	0.6638 (6)	0.1856 (4)
C(5)	0.368 (1)	0.5335 (8)	0.1236 (5)
C(6)	0.7740 (9)	0.5612 (6)	0.2414 (5)
C(7)	0.893 (1)	0.6152 (8)	0.1748 (6)
Ow	0.0733 (6)	0.1878 (4)	0.5711 (3)

(10) *International Tables For X-Ray Crystallography*; Kynoch Press: Birmingham, 1974; Vol. 4, pp 99–101, 149–150.
(11) Sheldrick, G. SHELX76, Program System for Crystal Structure Determination; University of Cambridge: Cambridge, 1976.
(12) Nardelli, M. *Comput. Chem.* **1983**, *7*, 95.
(13) Johnson, C. K. ORTEP Oak Ridge Natl. Lab. (Rep.). **1965**, ORNL-3794 programs, Oak Ridge, TN.

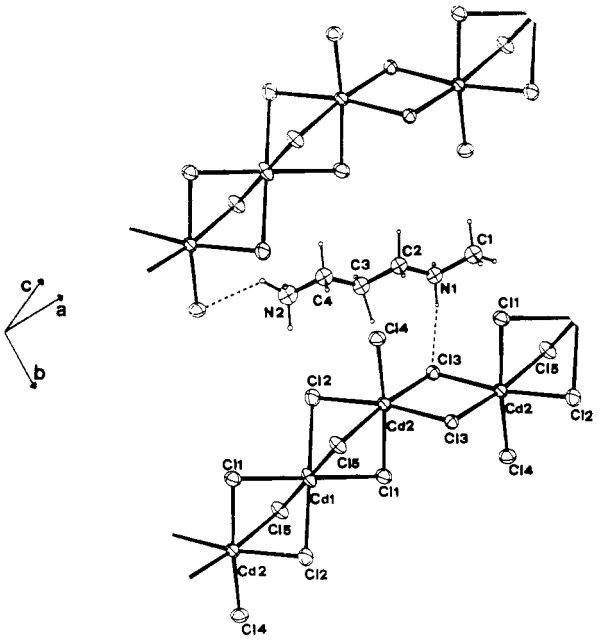

Figure 1. ORTEP view of the structure of $(mepnH_2)_2[Cd_3Cl_{10}]$ showing the atom numbering and thermal ellipsoid (40%) for the non-hydrogen atoms. The H atoms are represented as spheres of arbitrary radius.

Cl_{10}] form was done on an Italstructure goniometer, with Cu Kα (Ni filtered) radiation, with divergence aperture of 0.3° and receiving aperture of 0.1°.

Electrical Measurements. Fine powders obtained by grinding crystals of $(mepnH_2)_2[Cd_3Cl_{10}]$, $(et_2pnH_2)_2[Cd_5Cl_{14}]\cdot 2H_2O$, and $(et_2pnH_2)_2[Cd_5Cl_{14}]$ were compacted in vacuo under a pressure of 0.3 kN/mm to form disks of 28 mm in diameter and thickness up to 2 mm suitable for electrical measurements. The samples were then coated with gold by evaporation under vacuum with a proper electrode configuration and stored in a dark, vacuum environment over P_2O_5 until electrical measurements were made. Prior to any electrical measurements samples of $(mepnH_2)_2[Cd_3Cl_{10}]$ and anhydrous $(et_2pnH_2)_2[Cd_5Cl_{14}]$ were sintered under vacuum for 8 h at 160 and 140 °C, respectively: samples of $(et_2pnH_2)_2[Cd_5Cl_{14}]\cdot 2H_2O$ were measured as pressed. A three-terminal technique was used for both direct current (dc) and alternating current (ac) measurements, due to the rather low electrical conductivity exhibited by these compounds at room temperature. The voltmeter–ammeter method in dc and the Schering bridge method in ac measurements (10^{-2} Hz to 1 MHz), were used with cells and instrumentation elsewhere described,[14-16] according to ASTM D 150 and D 257 standards. Dc charging currents under an electric field of 1000 V cm^{-1} and discharging currents were also measured as a function of time to detect possible dielectric relaxation effects in the ultralow-frequency range by Fourier transform of the dc data.[17]

Results and Discussion

Crystal Structures of $(mepnH_2)_2[Cd_3Cl_{10}]$ and $(et_2pnH_2)_2[Cd_5Cl_{14}]\cdot 2H_2O$ Compounds. A drawing of the structure of both complexes showing the labeling scheme is reported in Figures 1 and 2. The most relevant bond distances and angles are summarized in Table IV and V.

Crystal structure of $(mepnH_2)_2[Cd_3Cl_{10}]$. The structure consists of infinite monodimensional polymeric chains of

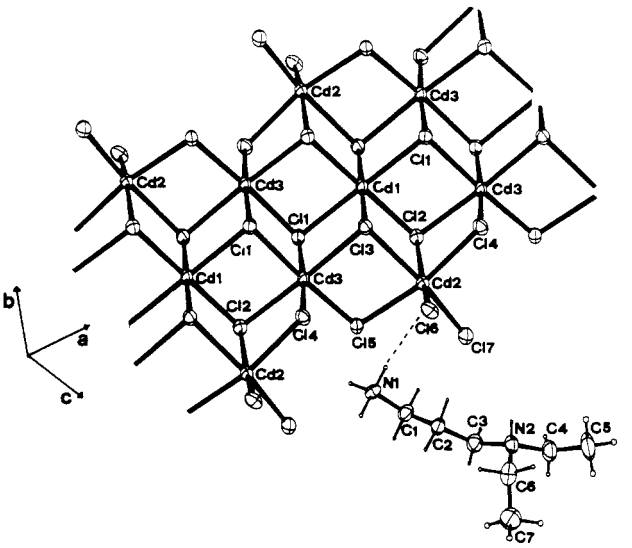

Figure 2. ORTEP view of the structure of $(et_2pnH_2)_2[Cd_5Cl_{14}]\cdot 2H_2O$ showing the atom numbering and thermal ellipsoid (40%) for the non-hydrogen atoms. The H atoms are represented as spheres of arbitrary radius.

Table IV. Bond Distances (Å) and Angles (deg) for the $(mepnH_2)_2[Cd_3Cl_{10}]$ (Esd's in Parentheses)[a]

Cd(1)–Cl(1)	2.628 (1)	Cd(2)–Cl(1)	2.609 (1)
Cd(1)–Cl(2)	2.546 (2)	Cd(2)–Cl(2)	2.733 (2)
Cd(1)–Cl(5)	2.799 (2)	Cd(2)–Cl(3)	2.623 (1)
Cd(1)···Cd(2)	3.425 (1)	Cd(2)–Cl(4)	2.500 (1)
Cd(2)···Cd(2)′	3.882 (1)	Cd(2)–Cl(5)	2.710 (1)
N(1)–C(1)	1.498 (7)	Cd(2)–Cl(3)′	2.695 (1)
N(1)–C(2)	1.486 (5)	C(2)–C(3)	1.525 (7)
N(2)–C(4)	1.483 (7)	C(3)–C(4)	1.506 (6)
Cl(2)–Cd(1)–Cl(5)	85.08 (6)	Cl(2)–Cd(2)–Cl(3)	173.58 (7)
Cl(1)–Cd(1)–C(5)	80.20 (6)	Cl(1)–Cd(2)–Cl(3)′	91.62 (6)
Cl(1)–Cd(1)–Cl(2)	85.93 (7)	Cl(1)–Cd(2)–Cl(5)	82.23 (6)
Cl(5)–Cd(2)–Cl(3)′	171.58 (8)	Cl(1)–Cd(2)–Cl(4)	172.50 (8)
Cl(4)–Cd(2)–Cl(3)′	90.23 (6)	Cl(1)–Cd(2)–Cl(3)	92.15 (6)
Cl(4)–Cd(2)–Cl(5)	95.16 (6)	Cl(1)–Cd(2)–Cl(2)	82.61 (6)
Cl(3)–Cd(2)–Cl(3)′	86.22 (6)	Cd(1)–Cl(1)–Cd(2)	81.70 (7)
Cl(3)–Cd(2)–Cl(4)	95.23 (7)	Cd(1)–Cl(2)–Cd(2)	80.33 (6)
Cl(3)–Cd(2)–Cl(5)	99.68 (6)	Cd(1)–Cl(5)–Cd(2)	76.87 (6)
Cl(2)–Cd(2)–Cl(5)	83.33 (6)	Cd(2)–Cl(3)–Cd(2)′	93.78 (6)
Cl(2)–Cd(2)–Cl(4)	90.12 (6)	C(1)–N(1)–C(2)	113.8 (4)
Cl(2)–Cd(2)–Cl(3)′	90.21 (6)	N(2)–C(4)–C(3)	108.9 (4)
C(2)–C(3)–C(4)	110.7 (4)	N(1)–C(2)–C(3)	109.1 (4)

[a] Single prime (′) = $-x + 1, -y, -z$.

$(Cd_3Cl_{10})_n^{4n-}$ moieties, running along the x axis, and of ammonium dications, anchoring two adjacent chains through hydrogen bonding interactions. Each Cd_3Cl_{10} unit is formed by a Cd(1) atom, lying on the symmetry center, coordinated by Cl(1), Cl(2), and Cl(5) atoms, which link the Cd(2) atoms forming three bridges; the coordination of each Cd(2) atom is completed by the terminal Cl(4) atom and by two symmetry-related Cl(3) atoms, bridging two Cd(2) atoms, respectively, the top and the end of two adjacent Cd_3Cl_{10} units. Each Cd atom shows an elongated octahedral geometry with Cd(1) and Cd(2) atoms in the trimer sharing a triangular face, while the octahedra formed by two Cd(2) atoms of adjacent trimers share the Cl(3)–Cl(3)′ edge. Bond lengths and angles are in agreement with the literature data.[2,6] However it is worth noting the spread of Cd(1)–Cl distances, observed in this compound (2.546 (2)–2.799 (1) Å), despite of the same bridging type of the three Cl atoms. The same three atoms furthermore bridge a Cd(2) atom in a more restricted range of distances (2.609 (1)–2.733 (2) Å).

(14) Sandrolini, F. *J. Phys. E: Sci. Instrum.* **1980**, *13*, 152.
(15) Sandrolini, F.; Cremonini, P. *Materie Plast. Elastomeri* **1979**, *7–8*, 405.
(16) Marrone, G.; Motori, A.; Nicolini, P.; Sandrolini, F. CIGRE, September 1992, Paper 15-402, Paris.
(17) Sandrolini, F. Proc. AIM Meeting on Electrical behaviour of polymeric materials, Bologna, Mar 1984, p 247.

Table V. Bond Distances (Å) and Angles (deg) for the $(et_2pnH_2)_2[Cd_5Cl_{14}]\cdot 2H_2O$ (Esd's in Parentheses)[a]

Cd(1)–Cl(1)	2.720 (1)	Cd(1)···Cd(3)	3.949 (1)
Cd(1)–Cl(2)	2.619 (1)	Cd(1)···Cd(2)	3.943 (1)
Cd(1)–Cl(3)	2.589 (1)	Cd(2)···Cd(3)	3.940 (1)
Cd(2)–Cl(2)	2.730 (1)	Cd(1)···Cd(3)′	3.967 (1)
Cd(2)–Cl(3)	2.797 (1)	Cd(2)···Cd(3)‴	3.995 (1)
Cd(2)–Cl(4)	2.690 (1)	Cd(3)···Cd(3)′	3.926 (1)
Cd(2)–Cl(5)	2.625 (1)	N(1)–C(1)	1.477 (8)
Cd(2)–Cl(6)	2.560 (2)	C(1)–C(2)	1.523 (8)
Cd(2)–Cl(7)	2.504 (1)	C(2)–C(3)	1.516 (8)
Cd(3)–Cl(1)	2.657 (1)	C(3)–N(2)	1.496 (8)
Cd(3)–Cl(2)	2.701 (1)	N(2)–C(4)	1.518 (8)
Cd(3)–Cl(4)	2.567 (1)	N(2)–C(6)	1.515 (8)
Cd(3)–Cl(1)′	2.672 (1)	C(4)–C(5)	1.512 (8)
Cd(3)–Cl(3)″	2.707 (1)	C(6)–C(7)	1.501 (8)
Cd(3)–Cl(5)″	2.530 (1)		
Cl(1)–Cd(1)–Cl(2)	84.93 (5)	Cl(1)′–Cd(3)–Cl(5)″	91.46 (5)
Cl(1)–Cd(1)–Cl(3)	95.21 (4)	Cl(2)–Cd(3)–Cl(3)″	175.37 (5)
Cl(2)–Cd(1)–Cl(3)	88.65 (4)	Cl(2)–Cd(3)–Cl(4)	86.05 (5)
Cl(2)–Cd(2)–Cl(3)	82.34 (4)	Cl(2)–Cd(3)–Cl(5)″	97.38 (5)
Cl(2)–Cd(2)–Cl(4)	83.12 (5)	Cl(3)″–Cd(3)–Cl(4)	98.20 (5)
Cl(2)–Cd(2)–Cl(5)	93.43 (5)	Cl(3)″–Cd(3)–Cl(5)″	84.31 (5)
Cl(2)–Cd(2)–Cl(6)	166.99 (5)	Cl(4)–Cd(3)–Cl(5)″	92.73 (5)
Cl(2)–Cd(2)–Cl(7)	91.61 (5)	Cd(1)–Cl(1)–Cd(3)	94.52 (5)
Cl(3)–Cd(2)–Cl(4)	88.10 (5)	Cd(1)–Cl(1)–Cd(3)′	94.74 (5)
Cl(3)–Cd(2)–Cl(5)	80.82 (5)	Cd(3)–Cl(1)–Cd(3)′	94.91 (5)
Cl(3)–Cd(2)–Cl(6)	88.49 (5)	Cd(1)–Cl(2)–Cd(3)	95.84 (5)
Cl(3)–Cd(2)–Cl(7)	169.89 (5)	Cd(1)–Cl(2)–Cd(2)	94.95 (5)
Cl(4)–Cd(2)–Cl(5)	168.75 (5)	Cd(2)–Cl(2)–Cd(3)	93.00 (5)
Cl(4)–Cd(2)–Cl(6)	87.40 (5)	Cd(1)–Cl(3)–Cd(2)	94.05 (4)
Cl(4)–Cd(2)–Cl(7)	99.25 (5)	Cd(1)–Cl(3)–Cd(3)‴	97.01 (5)
Cl(5)–Cd(2)–Cl(6)	94.19 (5)	Cd(2)–Cl(3)–Cd(3)‴	93.07 (5)
Cl(5)–Cd(2)–Cl(7)	91.52 (5)	Cd(3)–Cl(4)–Cd(2)	97.04 (5)
Cl(6)–Cd(2)–Cl(7)	98.71 (5)	Cd(2)–Cl(5)–Cd(3)‴	101.61 (5)
Cl(1)–Cd(3)–Cl(1)′	85.09 (5)	N(1)–C(1)–C(2)	109.3 (4)
Cl(1)–Cd(3)–Cl(2)	84.49 (5)	C(1)–C(2)–C(3)	109.8 (5)
Cl(1)–Cd(3)–Cl(3)″	93.48 (5)	C(2)–C(3)–N(2)	112.5 (5)
Cl(1)–Cd(3)–Cl(4)	90.77 (5)	C(3)–N(2)–C(4)	114.0 (4)
Cl(1)–Cd(3)–Cl(5)″	176.10 (5)	C(3)–N(2)–C(6)	111.1 (4)
Cl(1)′–Cd(3)–Cl(2)	92.19 (5)	C(4)–N(2)–C(6)	112.6 (4)
Cl(1)′–Cd(3)–Cl(3)″	83.45 (5)	N(2)–C(4)–C(5)	113.1 (5)
Cl(1)′–Cd(3)–Cl(4)	175.64 (5)	N(2)–C(6)–C(7)	112.8 (5)

[a] Single prime (′) = $-x - 1, -y, -z$; double prime (″) = $x - 1, y, z$; triple prime (‴) = $x + 1, y, z$.

In addition, the following structural features further distinguish Cd(1) from Cd(2): (i) bond distances at Cd(1) are slightly longer than those at Cd(2) (Table IV); (ii) metal–metal contacts between crystallographically independent atoms (intratrimer) are markedly shorter than those involving symmetry-related atoms (intertrimers): Cd(1)···Cd(2) = 3.425 (1) Å, Cd(2)···Cd(2)′ = 3.882 (1) Å; (iii) Cd(1) and Cd(2) are connected by three chlorine atoms and the Cd(1)–Cl(5)–Cd(2) angle (76.87 (6)°) is somewhat smaller with respect to those at Cl(1) and Cl(2). These are similar to one another and to those found for (pdH)-[$CdCl_3$] (78.72–81.74° range);[8] (iv) the short Cd(1)···Cd-(2) distance, due to the presence of three bridging chlorines, affects most of all the Cd(1)–Cl(5) distance which considerably increases; (v) the symmetry-related bridging Cl-(3) atoms give rise to an exactly planar ring with a Cd–Cl–Cd angle of 93.78°, as normally found in dibridged Cd atoms.[18]

The $mepnH_2$ dication is nearly planar and almost parallel to the polymeric chains; the N(1) hydrogen atoms interact with the Cl(3) of two different chains [N(1)···Cl-(3)′ = 3.213 (4) Å, H(4)···Cl(3)′ = 2.375 (1) Å, N(1)–H(4)···Cl-(3)′ = 143.9 (2)°; N(1)···Cl(3)″ = 3.212 (5) Å, H(5)···Cl(3)″ = 2.275 (1) Å, N(1)–H(5)···Cl(3)″ = 164.7 (3)°; single prime (′) = $-x, y - 1/2, z + 1/2$, double prime (″) = $x, y, z + 1$], while one N(2) hydrogen interacts with a terminal Cl(4) atom of one of the chain [N(2)···Cl(4)‴ = 3.218 (4) Å; H(12)···Cl(4)‴ = 2.449 (2) Å; N(2)–H(12)···Cl(4)‴ = 130.6 (8)°; triple prime (‴) = $-x, -y, -z$]. These contacts, although weak, contribute to the crystal packing.

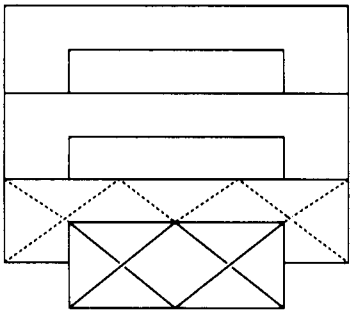

Figure 3. Stacking patterns of $(et_2pnH_2)_2[Cd_5Cl_{14}]\cdot 2H_2O$ compound.

Crystal structure $(et_2pnH_2)_2[Cd_5Cl_{14}]\cdot 2H_2O$. The structure contains alternate stacked pseudoplanar trinuclear $[Cd_3Cl_8]^{2-}$ and dinuclear $[Cd_2Cl_6]^{2-}$ units, organic dications and lattice water molecules. The Cd(1), lying on the symmetry center, is connected to two symmetry related Cd(2) atoms in the trimer through Cl(2) and Cl(3) and to two adjacent stacked dimers by Cl(1) atoms, which, also joining the two symmetry related Cd(3) atoms, form a perfectly planar Cd(3)Cl(1)Cd(3)′Cl(1)′ ring. All the coordination geometries around the Cd ions are distorted octahedra. In particular Cl(1), Cl(2), and Cl(3) atoms bridge three metal ions, belonging to stacked dimers and trimers, while the Cl(4) and Cl(5) atoms, bridging two cadmium(II) ions, join one dimer moiety to two adjacent trimers. This gives rise to polymeric endless ribbons running along the x axis. The Cd(1) is coordinated by six tribridged chlorine atoms; Cd(2) by two tribridged (Cl(2) and Cl(3)), two dibridged (Cl(4) and Cl(5)), and two terminal (Cl(6) and Cl(7)) chlorine atoms; Cd(3) by four tribridged and two dibridged chlorine atoms.

The $[Cd_2Cl_6]^{2-}$ anion is nearly planar with deviations of ±0.0472 Å, while in the $[Cd_3Cl_8]^{2-}$ anions the Cl atoms deviate significantly from the best plane (±0.1990 Å) with an angle of 6.91 (2)°. The resulting pattern is graphically represented in Figure 3. These patterns were introduced by Willett[19] in order to better visualize the great variety of stacking interactions to which halocuprates(II) can give rise. The $(et_2pnH_2)_2[Cd_5Cl_{14}]\cdot 2H_2O$ can be considered the first cadmium(II) compound in which stacking interactions among essentially planar moieties are found.

In the complex Cd–Cl distances vary according to the different bonding mode of the Cl atoms; their values normally increasing in the order terminal < dibridged < tribridged. The distortion from the regular octahedron is the greatest for Cd(2); the Cd(2)–Cl distances fall in a very large range (2.504 (1)–2.797 (1) Å) and the trans angles at Cd(2) markedly deviate from 180° (166.99 (5)–169.89 (5)°). The geometry distortion is progressively reduced for Cd(3) and Cd(1), being lowest for Cd(1) (Table V).

This structure presents a notably local symmetry degree, as is shown by the length of Cd···Cd contacts, which are very similar to one another in both intra- or interdinuclear and -trinuclear moieties.

(18) Ledesert, M. *Acta Crystallogr.* **1982**, *B38*, 1569.

(19) Geiser, U.; Willett, R. D.; Lindbeck, M.; Emerson, K. *J. Am. Chem. Soc.* **1986**, *108*, 1173–1179.

Only one weak hydrogen bond between the cation and the anionic tape chain [N(1)···Cl(6)′ = 3.232 (5) Å, H···Cl(6)′ = 2.348 (1) Å, N(1)–H(3)···Cl(6)′ = 140.0 (5)°; single prime (′) = $-x+1, -y+1, -z+1$] and a few weak contacts between the water oxygen and chlorine atoms (range 3.19–3.22 Å) are observed, suggesting that the chlorocadmate(II) ribbons are self-consistent and do not require strong stabilizing crystal-packing interactions.

Thermal and X-ray Powder Diffraction Results. The two compounds synthesized in this work exhibit very different thermal behavior. At increasing temperature, the hydrated $(et_2pnH_2)_2[Cd_5Cl_{14}]\cdot 2H_2O$ salt shows a loss of the lattice water molecules, which is complete in the temperature range 80–105 °C. The anhydrous form is stable up to 179 °C. At this temperature the compound simultaneously begins to melt and decompose. The dehydration process may be outlined as follows:

$$(et_2pnH_2)_2[Cd_5Cl_{14}]\cdot 2H_2O(sol) \xrightarrow{80\text{–}105\ ^\circ C} (et_2pnH_2)_2[Cd_5Cl_{14}](sol) + 2H_2O(g)$$

The experimental value from the DSC data for the heat of transformation (ΔH = 123.4 kJ/mol) is close to the one calculated for the dehydration heat of crystal hydrates (ΔH = 53.5–58.5 kJ/mol H_2O).[20,21] In this compound the hydrogen-bonding interactions among the chlorocadmate(II) ribbons, organic countercations, and water molecules are already rather weak at room temperature. Therefore on raising the temperature the subsequent increase of the thermal motion of the organic cations, together with the loss of the water molecules, further reduce these interactions, weakening the crystal packing. This is supported by the fact that this compound melts at a very low temperature (179 °C) if compared to other chlorocadmates (melting temperatures of about 270–290 °C). The dehydration reaction, however, does not affect the structure of the inorganic polymer. The local degree of symmetry and the strong inter- and intraoligomer associations of the chlorocadmates(II) may be considered to be majorly responsible for the stability of this compound up to the melting temperature.

The anhydrous $(mepnH_2)_2[Cd_3Cl_{10}]$ is thermally stable up to about 180 °C, where an endothermic event takes place, associated with a phase transition, which is completed at about 220 °C (ΔH = 20.2 kJ/mol). Repeated heating cycles between 30–230 °C performed on different samples demonstrated the reproducibility of this phase transition (Figure 4). The compound also presents a sharp endothermic peak, centered at 291 °C, corresponding to the melting point, after which it begins to decompose.

The phase transition seems to be of the first order, probably associated to the disordering of the hydrocarbon chains at higher temperatures. Since this induces some bulk structural change, in order to identify the crystalline phases of the $(mepnH_2)_2[Cd_3Cl_{10}]$ compound, the X-ray powder diffraction patterns for the low (named α) and high temperature (named β) phases are recorded. Those of polymorph β were tentatively indexed with the aid of TREOR,[22] a semiexhaustive trial-and-error powder indexing program. A total number of 22 lines was included

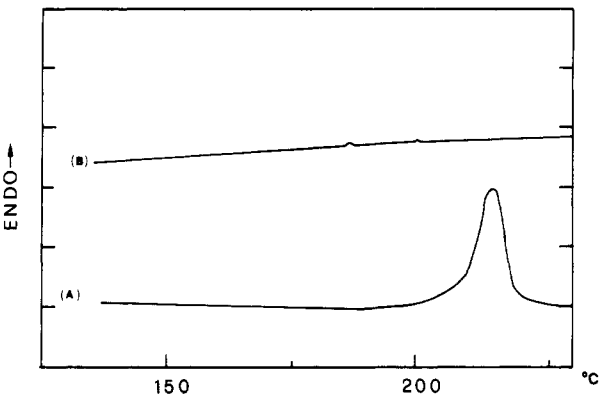

Figure 4. Heating (A)/cooling (B) cycles performed on the $(mepnH_2)_2[Cd_3Cl_{10}]$ compound.

Table VI. Indexed Powder Pattern for High-Temperature Phase $(mepnH_2)_2[Cd_3Cl_{10}]$ Compound

h	k	l	$2\theta_{obs}$	$2\theta_{calc}$
2	0	0	10.400	10.418
1	1	0	12.671	12.667
−2	0	1		12.710
−2	1	1	17.200	17.200
−1	0	2	17.488	17.490
2	1	1	18.450	18.452
−2	1	2	22.400	22.401
0	2	0	23.200	23.200
0	2	1		24.801
3	0	2	24.850	24.850
−3	1	2		24.868
5	0	0	26.250	26.238
			27.600[b]	
−1	1	3	28.550	28.549
−3	2	1		28.872
−3	0	3		28.873
4	0	2	28.950	28.929
2	0	3		29.401
−2	1	3	29.450	29.417
1	2	2	30.000	29.978
3	2	1		30.042
			30.700[b]	
−4	2	1	31.950	31.949
−5	1	2		32.003
−2	0	4	35.400	35.404
5	1	2		35.456
−2	2	3		35.863
6	1	1	35.900	35.903
2	3	0	36.700	36.720
−3	0	4		36.758
−5	2	2	38.050	38.059

[a] a = 17.097 Å; b = 7.662 Å; c = 10.296 Å; β = 97.02. [b] Observed but unexplained reflections by the proposed tentative cell.

in the set of identifiable reflections. The monoclinic unit cell a = 17.10, b = 7.66, c = 10.30 Å, β = 97.0°, V = 1338.6 Å^3 showed a satisfactory agreement between observed and calculated positions on the 2θ scale with the figures of merit M_{20}[23] and F_{20}[24] which are 12 and 19 respectively and two (weak) peaks unindexed. The lower calculated density of polymorph β (2.17 g/cm^3) is in agreement with the hypothesis that some disordering is the event responsible for the $\alpha \rightarrow \beta$ transition. The absence of $h0l$ with l odd and $0k0$ with k odd for the β form also suggests the same $P2_1/c$ space group (Table VI). We point out, however, that the indexing process, in the case of a low-symmetry system, is difficult, and the suggested unit cell is to be considered as tentative.

The reversibility of the $\alpha \rightarrow \beta$ transition, which is completed in three weeks, had been tested with the aid of

(20) Dei, L.; Guarini, G. G. T.; Piccini, S. *J. Thermal. Anal.* **1984**, *29*, 755.
(21) Giusti, J.; Guarini, G. G. T.; Menabue, L.; Pellacani, G. C. *J. Thermal Anal.* **1984**, *29*, 639.
(22) Werner, P. E.; Eriksson, L.; Westdahl, M. *J. Appl. Crystallogr.* **1985**, *18*, 367.
(23) De Wolff, P. M. *J. Appl. Crystallogr.* **1968**, *1*, 108.
(24) Smith, G. S.; Synder, R. L. *J. Appl. Crystallogr.* **1979**, *12*, 60.

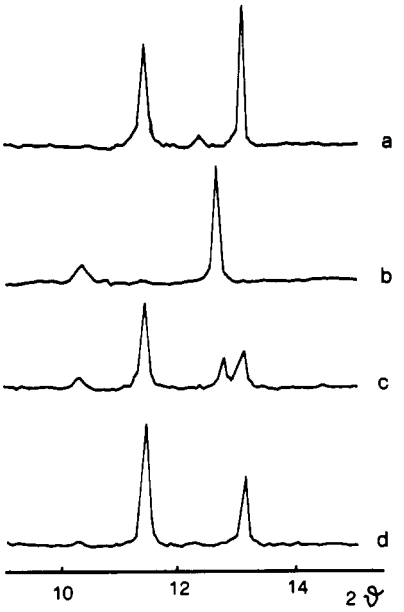

Figure 5. Diffraction profiles of the $(mepnH_2)_2[Cd_3Cl_{10}]$ compound collected at room temperature (pure α polymorph) (a), at 230 °C (b) (almost pure β polymorph), after cooling at room temperature and keeping for 2 weeks (c) (copresence of both α and β forms) and three weaks (d) (almost complete change back to the α polymorph).

X-ray powder diffraction patterns. Results are reported in Figure 5 where the diffraction profiles of the same sample collected at different stages of its thermal history are reported. Profile (a) corresponds to the initial α polymorph; profile (b) is obtained after keeping the samples for 30 min at 230 °C and correspond to almost pure β polymorph; profile (c) is obtained after keeping the sample for two weeks at room temperature and shows the copresence of both α and β peaks, while profile (d), collected after 3 weeks (at room temperature), shows an almost complete change back to the α polymorph. The different intensities of the peaks at $2\theta = 11.5°$ and 13.2° observed in patterns (a) and (d), respectively, are not meaningful since small preferred orientation effects could be invoked as a possible explanation for this difference.

Far-Infrared Spectra. The IR spectrum of the $(et_2pnH_2)_2[Cd_5Cl_{14}]\cdot 2H_2O$ compound in the 4000–250-cm^{-1} region shows a great number of very sharp absorption bands, indicating a high degree of symmetry, which remains after dehydration of the compound. The IR spectrum of the anhydrous form differs from that of the hydrated only by reason of the disappearance of water absorptions and the shift at higher energies (about 30 cm^{-1}) of the NH^+ and NH_3^+ stretching and bending vibrations. This again confirms that the loss of water molecules decreases the already-weak hydrogen bonding interactions.

In the far-IR spectra (400–60 cm^{-1}) the hydrated et_2pnH_2 salt shows a very broad band centered at 183 cm^{-1}, with a shoulder at 206 cm^{-1}, assignable to the bridging and terminal Cd–Cl stretching vibrations, respectively. In the anhydrous form the weakening of the hydrogen bonding interactions separates the Cd–Cl stretching vibrations, which appear as well distinguishable sharp peaks at 162 and 212 cm^{-1}, respectively.

No remarkable differences are observed in shape and position bands in the IR spectra of the α and β $(mepnH_2)_2[Cd_3Cl_{10}]$ forms in the 4000–250-cm^{-1} range. The far-IR spectra of the α and β forms of the $(mepnH_2)_2[Cd_3Cl_{10}]$ compound are very similar, showing the terminal and bridging Cd–Cl stretching vibrations at 249 and 179 cm^{-1}, respectively, confirming the hypothesis that the $\alpha \rightarrow \beta$ transition does not affect the inorganic chains.

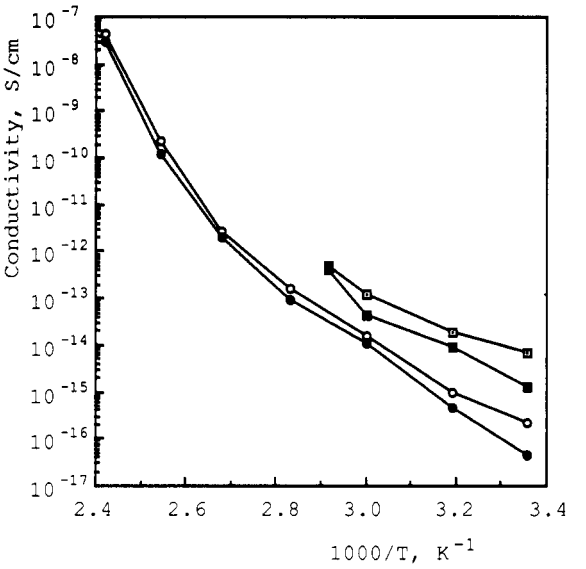

Figure 6. Electrical conductivity σ of $(et_2pnH_2)_2[Cd_5Cl_{14}]\cdot 2H_2O$ (□) and $(et_2pnH_2)_2[Cd_5Cl_{14}]$ (○) as a function of reciprocal absolute temperature at 1 (○, □) and 60 (●, ■) minutes after the voltage application.

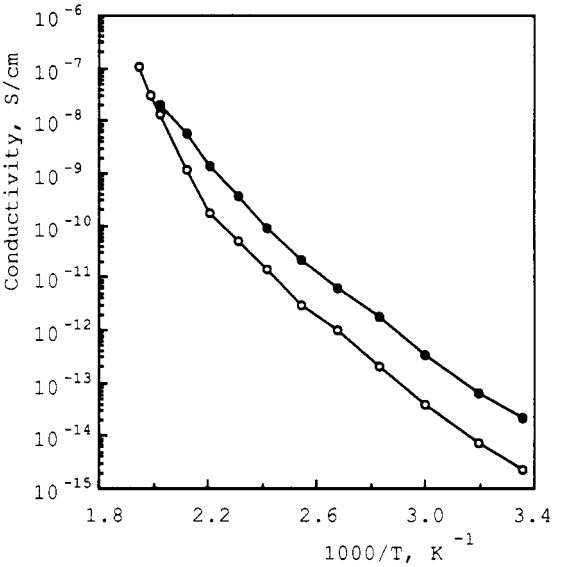

Figure 7. Electrical conductivity σ of $(mepnH_2)_2[Cd_3Cl_{10}]$ as a function of reciprocal absolute temperature at 10 minutes after the voltage application: (○) heating cycle; (●) cooling cycle.

Electrical Results. Figure 6 reports the electrical conductivity σ calculated at 1 and 60 min after the voltage application for the hydrated and anhydrous et_2pnH_2 compounds as a function of the reciprocal absolute temperature, in the temperature range 25–160 °C. The dc behavior in the Arrhenius plot is not linear, and transient phenomena are present in both compounds. Figure 7 shows the electrical conductivity of $(mepnH_2)_2[Cd_3Cl_{10}]$ in the temperature range 25–240 °C. As no meaningful transient phenomena were found, data at 10 min only are reported. Measurements were performed from room temperature to 240 °C and subsequently repeated from this temperature to 25 °C in order to detect any possible change induced by phase transition. At a temperature

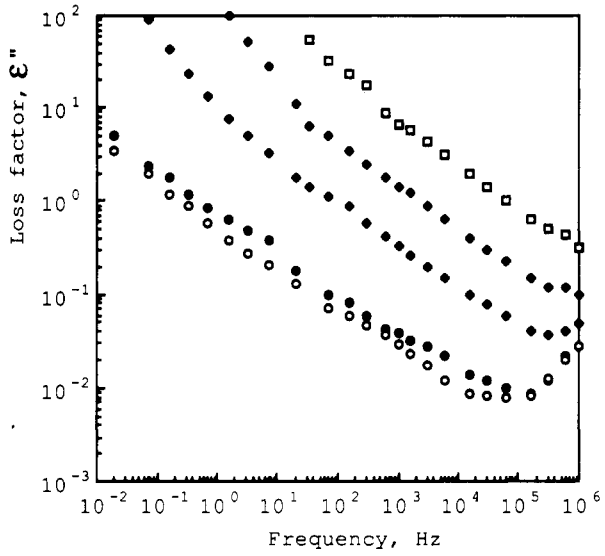

Figure 8. Loss factor of $(et_2pnH_2)_2[Cd_5Cl_{14}]$ vs frequency at variable temperature [T = 125 (□), 100 (◆), 75 (◇), 50 (●), 25 °C (○)].

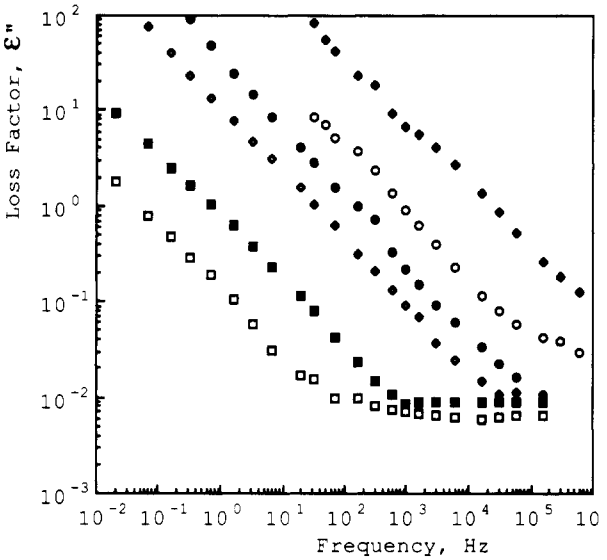

Figure 9. Loss factor of $(mepnH_2)_2[Cd_3Cl_{10}]$ vs frequency at variable temperature [T = 200 (◆), 150 (○), 125 (●), 100 (◇), 50 (■), 25 °C (□)].

close to 180 °C a change in the slope of conductivity vs temperature takes place (apparent average activation energy below 180 °C: 78 kJ/mol). Subsequently, as temperature is decreased, an hysteresis cycle takes place, conductivity being higher than during the increasing of temperature. It is worth noting, however, that the apparent activation energy remains the same. Measurements performed at room temperature on samples of $(mepnH_2)_2[Cd_3Cl_{10}]$ after the absorption of a slight amount of moisture, showed a strong increase of conductivity (about 6 orders of magnitude for an absorption of about 3 wt % of water moisture). As found for similar compounds,[7-9,26] $(mepnH_2)_2[Cd_3Cl_{10}]$ and $(et_2pnH_2)_2[Cd_5Cl_{14}]$ can be classified as insulators at room temperature. However, their conductivities strongly increase with temperature and reach values in the semiconducting range at the highest temperatures.

Dielectric measurements in the frequency range 10^{-2}–10^6 Hz at constant temperatures showed no remarkable relaxation effects (Figures 8 and 9). The relative dielectric constants (not reported for sake of brevity) increase with temperature and decrease with frequency at all the investigated temperatures: at the highest frequencies, as temperature increases, values span from 8 to 10 for $(mepnH_2)_2[Cd_3Cl_{10}]$ and from 6 to 8 for $(et_2pnH_2)_2[Cd_5Cl_{14}]$. Loss factors of both compounds at constant temperature increase with decreasing frequency, the one of $(et_2pnH_2)_2[Cd_5Cl_{14}]$ being lower at temperatures below 80 °C but higher than that of $(mepnH_2)_2[Cd_3Cl_{10}]$ at temperatures over 100 °C according to dc results. The Fourier transform of the discharging current showed no relaxation processes of the Maxwell–Wagner–Sillars type.

As found for the analogous chlorocadmates previously studied,[7-9,25] the whole electrical behavior of $(mepnH_2)_2[Cd_3Cl_{10}]$ and $(et_2pnH_2)_2[Cd_5Cl_{14}]$ seems to hint to an ionic mechanism of conduction, particularly at high temperatures. A large increase in conductivity is caused by moisture absorption, anhydrous $(et_2pnH_2)_2[Cd_5Cl_{14}]$ exhibits a lower conductivity at room temperature than its hydrated form, the slope of loss factor as a function of frequency in a log–log plot tends to unity at high temperatures. Protons are supposed to be the charge carriers by migration through the hydrogen bonds, a mechanism similar to that found in some hydrogen bonded systems.[26,27] Of course, an electronic mechanism cannot be excluded to contribute to the electrical conduction processes especially at low temperatures. Two more features must be highlighted: (i) values of $(et_2pnH_2)_2[Cd_5Cl_{14}]$ conductivity increase by 5 orders of magnitude from 80 to 140 °C, a much higher change than those observed in other chlorocadmates: this can be explained by the weakening of the lattice structure that takes place after dehydration, which may favor proton migration through the lattice at high temperatures (ii) the change in the slope of conductivity vs temperature found in $(mepnH_2)_2[Cd_3Cl_{10}]$ (an effect already found in other chlorocadmates[25]) is to be related to the phase transition already mentioned: the nonreproducibility of conductivity as temperature is lowered agrees with the apparent irreversibility of the $\alpha \rightarrow \beta$ transition. The increase in conductivity, exhibited on cooling, is to be related to the appearance of the less dense, less compact β phase, which again may favor proton migration.

Conclusions

The structures of the investigated compounds are rather unusual and until now have never been found for chlorocadmates(II) as demonstrated in comparison with the known 1-D polymeric species.[6,8,9,28] The hydrogen-bonding capabilities and steric hindrances of the organic countercations may be considered the major factors responsible in determining the polymeric characteristics of the chlorocadmates. In the presence of unsubstituted diprotonated diamines, such as ethylenediamine[25] and propane-1,3-,[29] butane-1,4-, and pentane-1,5-diamine,[30,31] etc., a

(25) Battaglia, L. P.; Bonamartini Corradi, A.; Pelosi, G.; Cramarossa, M. R.; Manfredini, T.; Pellacani, G. C.; Motori, A.; Saccani, A.; Sandrolini, F.; Brigatti, M. F. *Chem. Mater.* **1992**, *4*, 813.

(26) Seanor, D. A. *J. Polym. Sci.* **1968**, *6*, 463.
(27) Weller, M. T.; Bell, R. G. *Solid State Ionics* **1989**, *35*, 79.
(28) Wei, C. S. *Acta Crystallogr. C43*, **1987**, 2295.
(29) Willett, R. D. *Acta Crystallogr.* **1977**, *B33*, 1641.
(30) Kind, R.; Plesko, S.; Gunter, P.; Roos, J.; Fousek, J. *Phys. Rev.* **1981**, *B23*, 5301 and references therein.

bidimensional structure of the chlorocadmates(II) invariably results, consisting of sequences of alternating layers of corner-sharing ($CdCl_6$) octahedra (perovskite-type structure). Adjacent layers are anchored by interposed sheets of aligned dications, in the extended form, which stabilize the structure through strong hydrogen bonding interactions.

When mono- or disubstituted propane-1,3-diamine are present, as in the case of $mepnH_2$ or et_2pnH_2, the lowered hydrogen-bonding capabilities and the increased disorder and steric effects, if compared to the corresponding unsubstituted diamines, seem to favor the formation of 1-D polymeric chlorocadmates(II). However, it is not possible to predict a priori the exact polymerization patterns. The results of this paper indicate that cations with the lowest hydrogen-bonding abilities and greatest steric effects may favor polymeric ribbons more than strictly 1-D endless single chains. The different bridging capabilities of the chlorine atoms are responsible for the great variety of essentially 1-D structural archetypes.

Noteworthy for the $(mepnH_2)_2[Cd_3Cl_{10}]$ compound is the presence at about 180 °C of an unusually slow reversible first-order phase transition, which is pointed out by thermal, electrical or X-ray powder diffraction measurements. This transition is associated to the disordering of the hydrocarbon chains, which gives rise to a lower dense β form.

The electrical conductivity of the investigated compounds is essentially ionic, likely by protons migration via hydrogen bonds. The presence of a network of very weak hydrogen bonding among the inorganic and organic species and the reduced density of the β phase for $(mepnH_2)_2[Cd_3Cl_{10}]$ compound may favor such a mechanism and increase the electrical conductivity. The whole electrical behavior can thus be consistently related with structure and phase changes occurring in the investigated compounds.

Acknowledgment. Financial support (60%) of the MURST and Italian Consiglio Nazionale delle Ricerche (CNR) is gratefully acknowledged.

Supplementary Material Available: Tables of anisotropic and isotropic temperature factors and positional and thermal parameters for hydrogen atoms (4 pages); list of observed and calculated structure factors for $(mepnH_2)_2[Cd_3Cl_{10}]$ and for $(et_2pnH_2)_2[Cd_5Cl_{14}]$ compounds (16 pages). Ordering information is given on any current masthead page.

(31) Negrier, P.; Chanh, N. B.; Courseille, C.; Hauw, C.; Meresse, A.; Couzi, M. *Phys. Status Solidii A*, 1987, *100*, 473.